

## Supporting Information

### Title

### **Photo-switchable Electron-transporting Layers for Self-driven Perovskite Photodetectors towards High Detectivity**

*Qinglei Zhang<sup>†</sup>, Meihua Shou<sup>†</sup>, Yucheng Xu<sup>†</sup>, Jiabin Zheng<sup>†</sup>, Xinbo Wen<sup>†</sup>, Yang Zhao<sup>‡</sup>, Huan Wang<sup>\*‡</sup>, Linlin Liu<sup>\*†</sup>, and Zengqi Xie<sup>\*†</sup>*

<sup>†</sup>State Key Laboratory of Luminescent Materials and Devices, Institute of Polymer Optoelectronic Materials and Devices, Guangdong Provincial Key Laboratory of Luminescence from Molecular Aggregates, South China University of Technology, Guangzhou 510640, P. R. China.

Email: [mliull@scut.edu.cn](mailto:mliull@scut.edu.cn), [msxiez@scut.edu.cn](mailto:msxiez@scut.edu.cn).

<sup>‡</sup>College of Chemistry and Chemical Engineering, Northeast Petroleum University, Daqing 163318, China.

Email: [wanghuan83214@gmail.com](mailto:wanghuan83214@gmail.com)

## Table of Contents:

1. Calculation of energy level for ZnO:PBI-H .....	S3
2. Calculation of mobility .....	S3
3. Absorption, PL and UPS spectra .....	S4
4. Cross-section SEM image of Device B .....	S5
5. Optimization of PEIE layer .....	S5
5.1 Photographs of perovskite films on different substrates .....	S5
5.2 AFM images of perovskite on different substrates .....	S7
5.3 SEM images .....	S9
5.4 The photocurrent and dark current density of devices with varied PEIE layer .....	S10
5.5 Charge and discharge characteristics .....	S11
6. Mobility measurement .....	S12
6.1 $I_D$ - $V_G$ curves used to calculate charge carrier mobility .....	S12
6.2 Clear observation of $I_D$ - $V_G$ curves in dark and under light .....	S13
7. Contrast of fall time and schematic diagram for the charge transfer .....	S13
8. Response speed of devices with different active area .....	S14
9. Summary of perovskite photodetectors with varied concentration of PEIE .....	S14
10. References .....	S15

## 1. Calculation of energy level for ZnO:PBI-H

The energy level was calculated as reported before.<sup>S1</sup> The Fermi level ( $E_f$ ) was -3.70 eV, and the valence band maximum (VBM) was -7.19 eV obtained from Fig. S1b and Fig. S1c, which was 3.49 eV lower than  $E_f$ . As shown in Fig. S1d, the band gap ( $E_g$ ) of ZnO:PBI-H was calculated to be 3.22 eV, which was similar to ZnO. The conduction band minimum (CBM) was calculated to be -3.97 eV according to  $CBM = VBM + E_g$ .

## 2. Calculation of mobility

For FET devices, at the source-drain voltage ( $V_D$ ) equals to 20 V, the mobility was calculated

by  $I_D = \frac{W}{L} \mu C_i (V_G - V_T) V_D$  in the linear region, where  $I_D$  is the source-drain current,  $W$  is the channel width,  $L$  is the channel length,  $\mu$  is the mobility,  $C_i$  is the capacitance of dielectric layer (silicon dioxide 11.7 nF·cm<sup>-2</sup>),  $V_G$  is the gate voltage and  $V_{th}$  is the threshold voltage.

### 3. Absorption, PL and UPS spectra

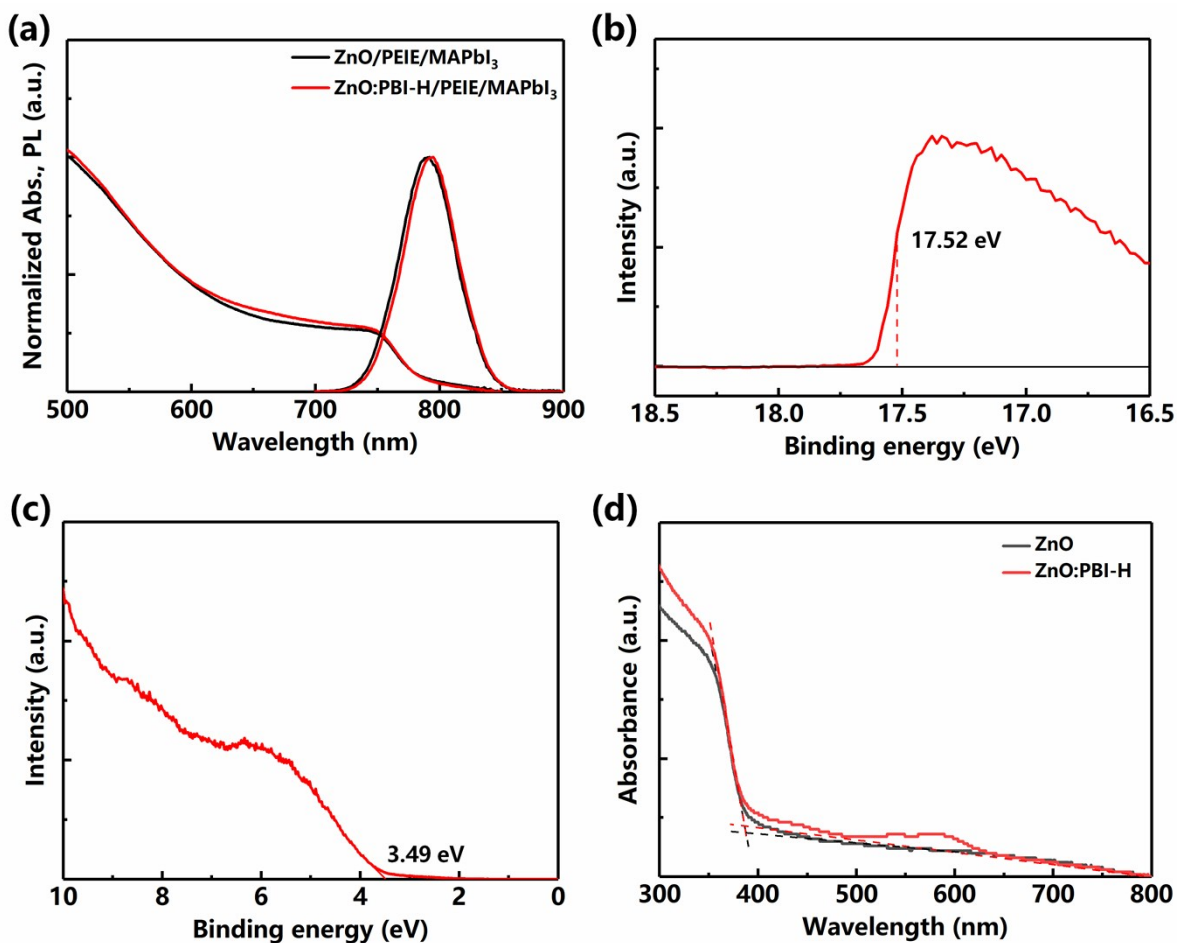


Fig. S1 (a) Normalized absorption and photoluminescence spectra of ZnO/PEIE/MAPbI<sub>3</sub> (black) and ZnO:PBI-H/PEIE/MAPbI<sub>3</sub> (red), in which the concentration of PEIE was 0.2 wt%; (b) Photoemission cutoff and (c) the Fermi edge obtained via ultraviolet photoelectron spectroscopy (UPS) for ZnO:PBI-H; (d) The absorption spectra of ZnO and ZnO:PBI-H.

#### 4. Cross-section SEM image of Device B

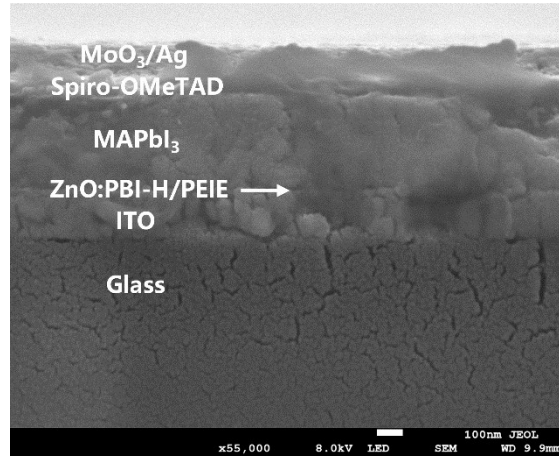


Fig. S2 Cross-sectional scanning electron microscopy (SEM) image of Device B.

#### 5. Optimization of PEIE layer

##### 5.1 Photographs of perovskite films on different substrates

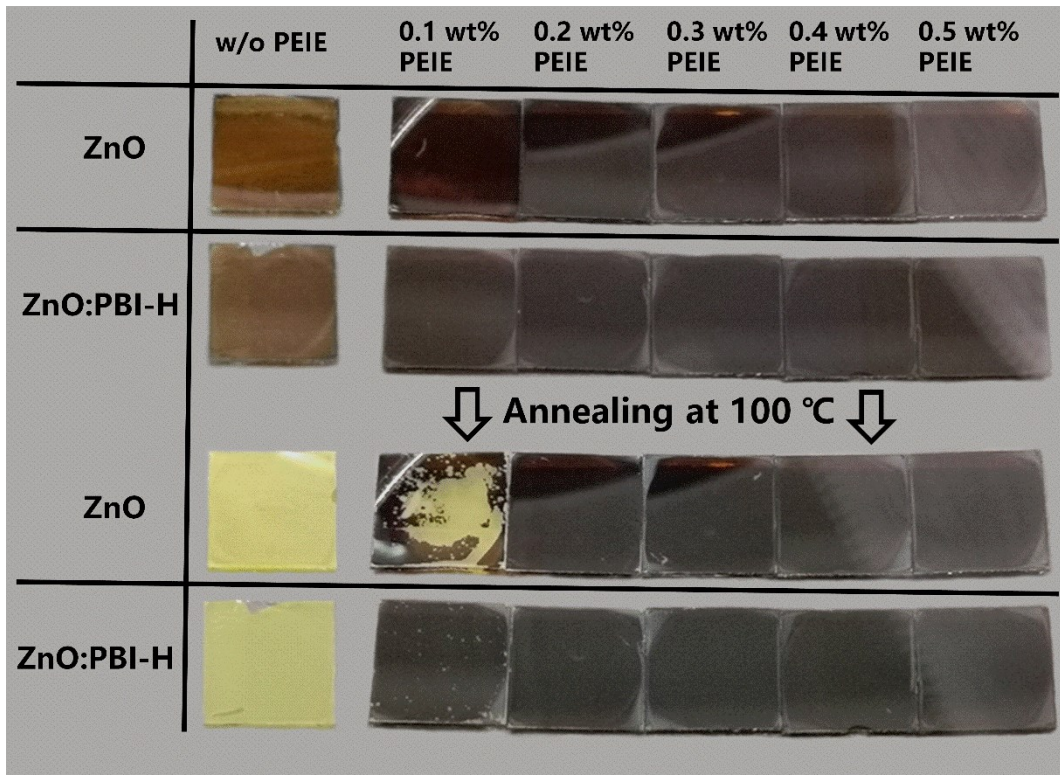


Fig. S3 Photographs of perovskite films on ZnO and ZnO:PBI-H with different concentration of PEIE as interlayers before annealing (top) and after annealing (bottom).

The perovskite films prepared on substrates were all heated at 60 °C for 2 minutes which all remained black meaning no decomposition of perovskite at such low temperature except those without PEIE layer. After annealing at 100 °C for 20 minutes, for those without PEIE layer in which perovskite contacted directly with ZnO or ZnO:PBI-H, the whole surface area turned yellow which indicated the perovskite had decomposed for their extreme sensitivity to high temperature. If the PEIE layer was too thin (e.g. from the 0.1 wt% PEIE solution), the ZnO or ZnO:PBI-H could only be covered partially, while when the concentration was 0.2 wt% or higher, ZnO (or ZnO:PBI-H) and MAPbI<sub>3</sub> could be well separated by the PEIE layer, which means that PEIE played an important role in separating perovskite from ZnO (or ZnO:PBI-H) and avoiding the decomposition of perovskite. It seemed that the PBI-H doped ZnO might act partly on inhibiting the decomposition of perovskite, because the perovskite on ZnO:PBI-H/0.1 wt% PEIE showed almost black with several yellow spots compared to that on ZnO/0.1 wt% PEIE.

## 5.2 AFM images of perovskite on different substrates

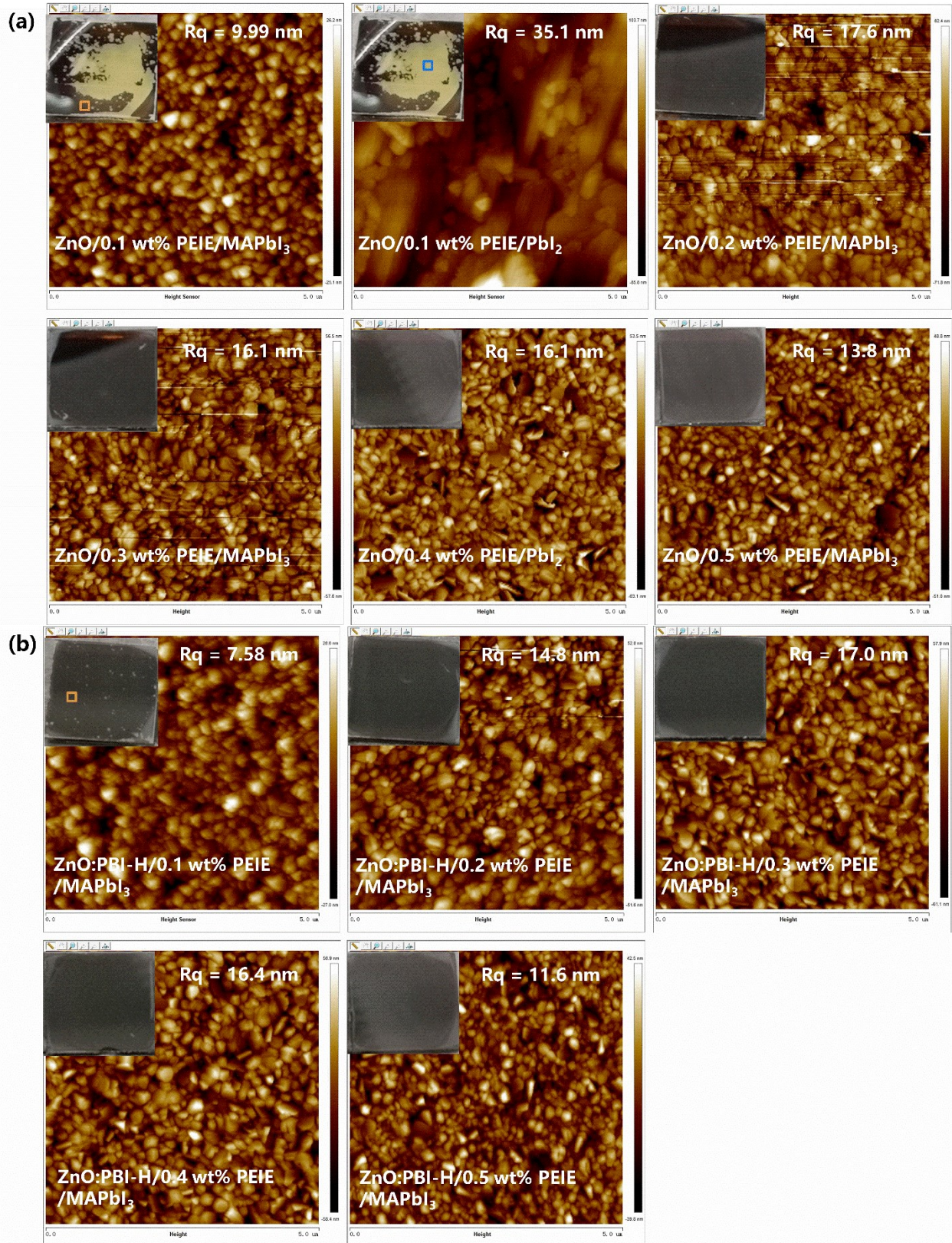


Fig. S4 Atomic force microscopy (AFM) images of perovskite deposited on (a) ZnO and (b) ZnO:PBI-H covered by PEIE from various concentration of solutions. The insets are the photographs of corresponding perovskite films and root-mean-square roughness ( $R_q$ ), in which the red squares and blue squares are the scanning areas of black phases and yellow phases, respectively.

Fig. S4 shows that though the thin PEIE layer fabricated from 0.1 wt% solution could partly cover the ZnO or ZnO:PBI-H layer, the crystallization of perovskite based on that was obviously poorer than that on 0.2 wt% PEIE. Even if the whole area of perovskite on ZnO:PBI-H/0.1 wt% PEIE kept almost black phases, the crystallization of perovskite showed quite poor morphology with plenty of small particle-like crystalline grains which was the same as the black phases of perovskite on ZnO/0.1 wt% PEIE. The morphologies for ZnO (or ZnO:PBI-H)/0.2 wt% PEIE/ $\text{CH}_3\text{NH}_3\text{PbI}_3$  ( $\text{MAPbI}_3$ ) represented typical perovskite film structure with larger and more compact crystalline grains, implying better performance.

### 5.3 SEM images

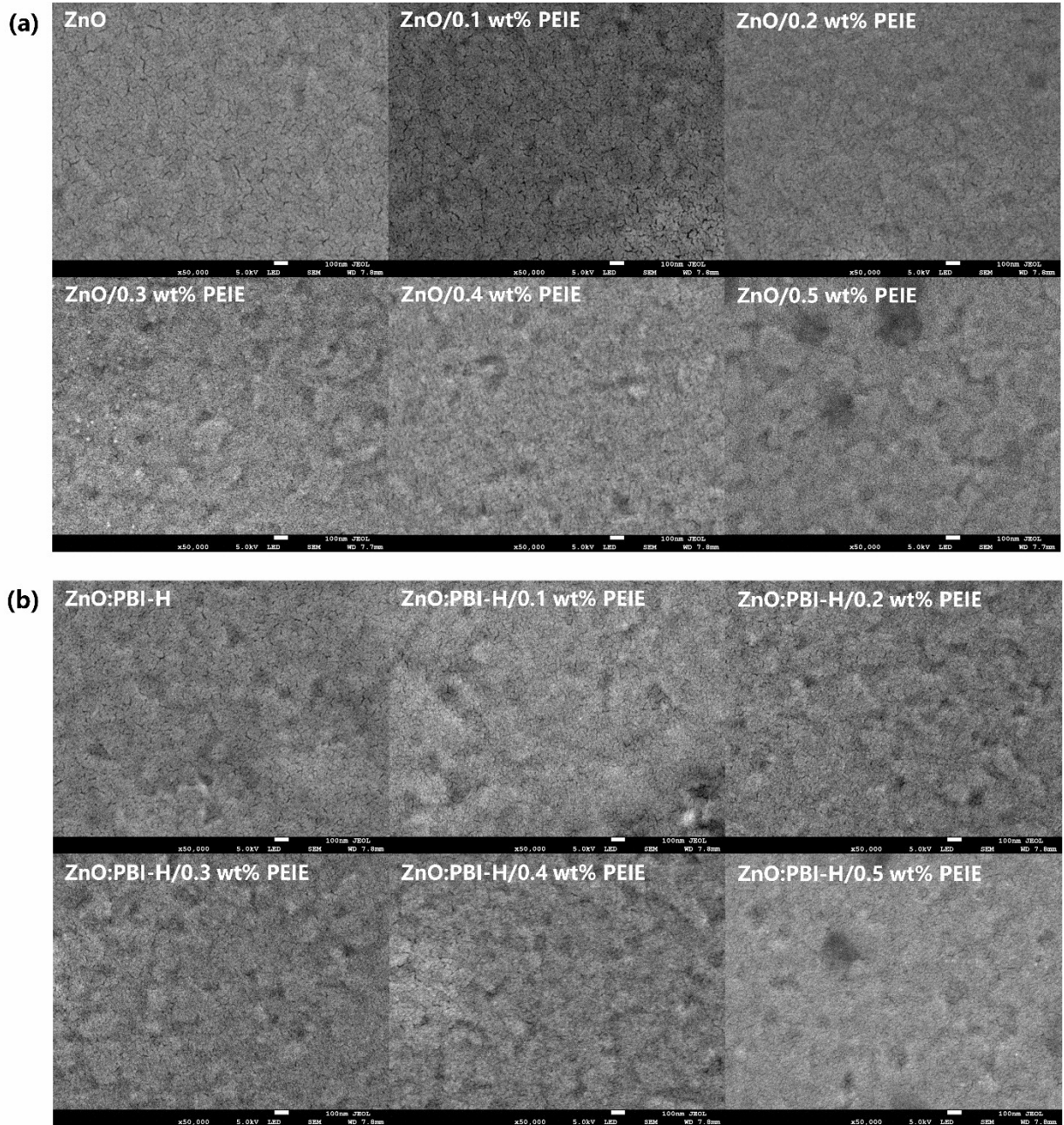


Fig. S5 SEM images of (a) ZnO and (b) ZnO:PBI-H covered with PEIE from varied concentration (0.1 wt% to 0.5 wt%).

## 5.4 The photocurrent and dark current density of devices with varied PEIE layer

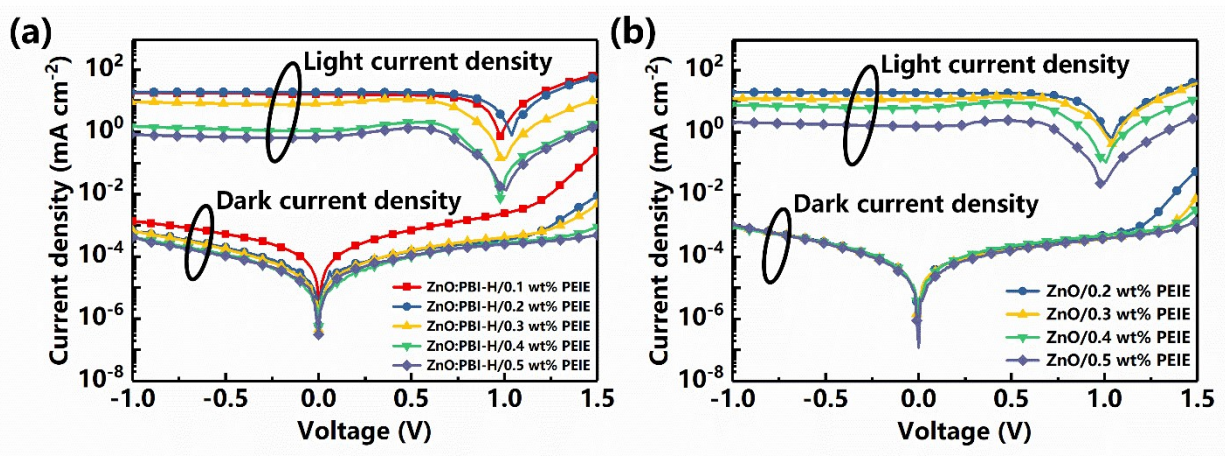


Fig. S6 The photocurrent and dark current density of perovskite photodetectors with (a) ZnO:PBI-H and (b) ZnO as the electron-transporting layer, in which the concentration of PEIE precursor solution varies from 0.1 to 0.5 wt% for ZnO:PBI-H based devices and from 0.2 to 0.5 wt% for ZnO based devices, respectively.

With a low concentration of 0.2 wt% PEIE that the formed interlayer was just enough to separate perovskite from ZnO (or ZnO:PBI-H), the photocurrent was as high as  $18.7 \text{ mA}\cdot\text{cm}^{-2}$  similar to ZnO based perovskite solar cells; but when the concentration reached 0.3 wt% or higher, the photocurrent in both ZnO and ZnO:PBI-H based devices presented an evident decline which was caused by the poor conductivity of PEIE. The key performance parameters of perovskite photodetectors with different interfacial layers are shown in Table S1. With the increased concentration of PEIE, the dark current density of perovskite photodetectors kept almost unchanged, while the photocurrent density and responsivity declined evidently leading to the low detectivity.

## 5.5 Charge and discharge characteristics

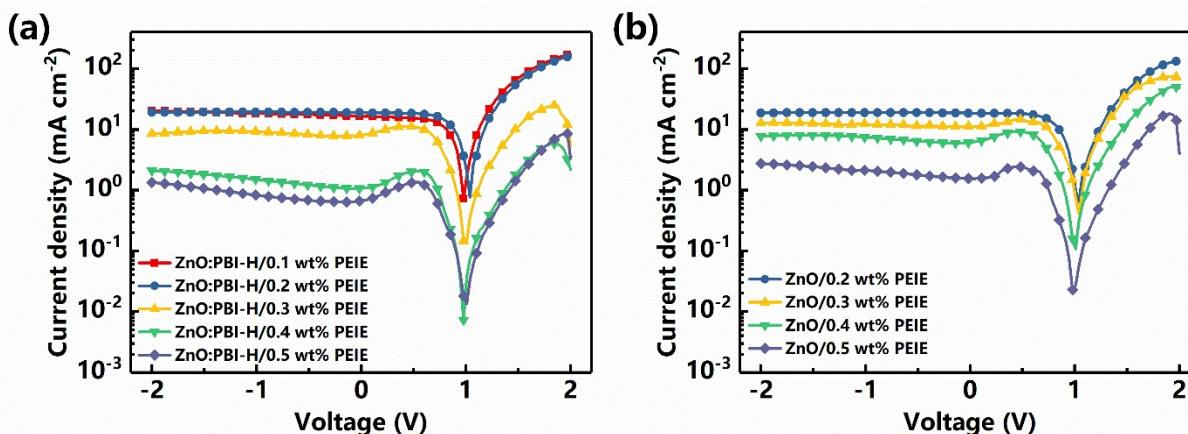


Fig. S7 The photocurrent of perovskite photodetectors based on (a) ZnO:PBI-H and (b) ZnO with different concentration of PEIE precursor solution (0.1-0.5 wt% for the former, 0.2-0.5 wt% for the latter, respectively).

At the concentration of PEIE being higher than 0.3 wt%, there would be charge storage in devices. When the forward bias swept from 2 V to low count, the photocurrent became firstly smaller and then larger, which was corresponding to the charge storage. When the forward bias dropped to about 0.5 V, the charges stored before were released to generate a slightly gradual increase in the reverse current. The modest photocurrent density indicated that the thick PEIE layer would hinder the charge transport, though it could better separate perovskite from ZnO (or ZnO:PBI-H). Thus, the Device A and Device B were all fabricated from 0.2 wt% PEIE solution.

## 6. Mobility measurement

### 6.1 $I_D$ - $V_G$ curves used to calculate charge carrier mobility

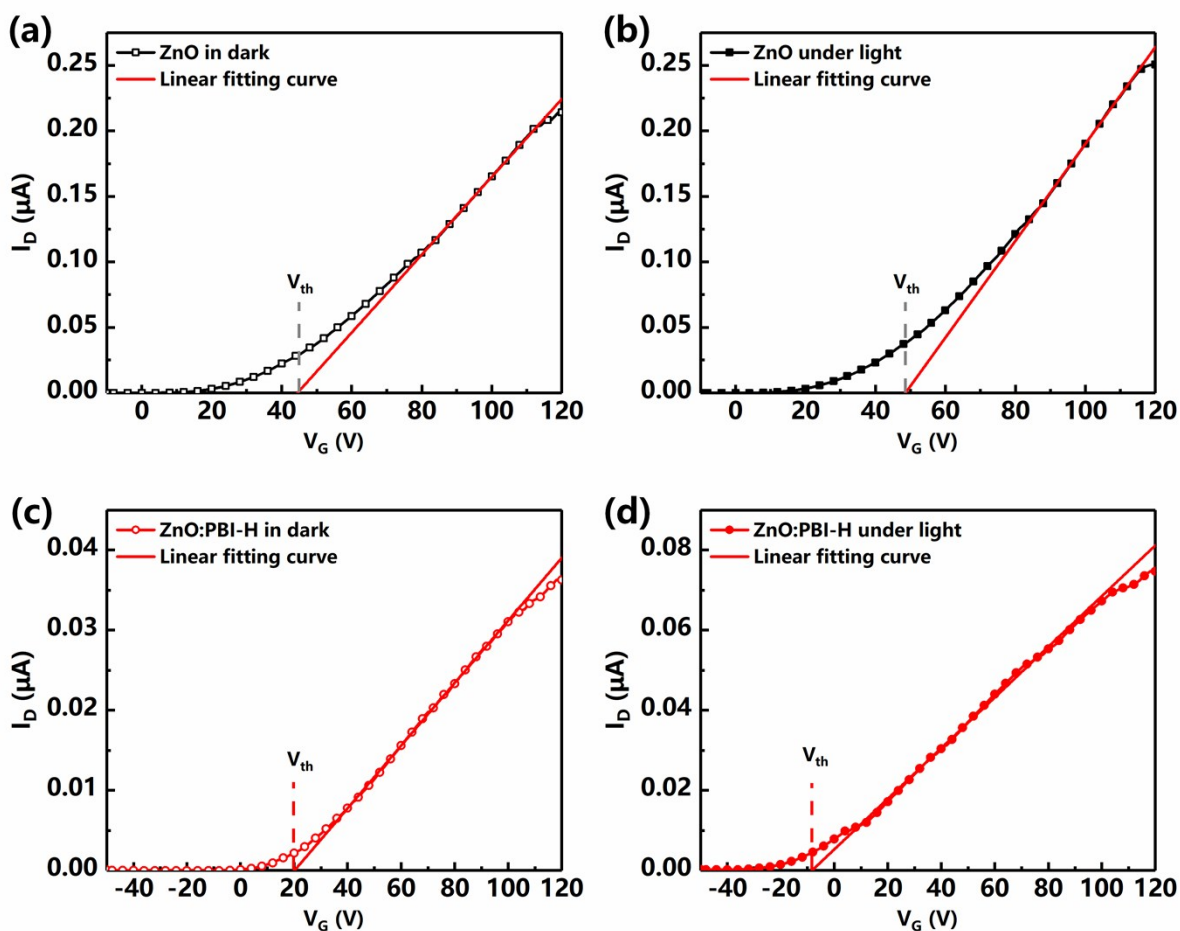


Fig. S8 Source-drain current versus gate voltage of (a) ZnO in dark (hollow square), (b) ZnO under light (solid square), (c) ZnO:PBI-H in dark (hollow circle) and (d) ZnO:PBI-H under light (solid circle) respectively. The source-drain voltage is 20 V.

## 6.2 Clear observation of $I_D$ - $V_G$ curves in dark and under light

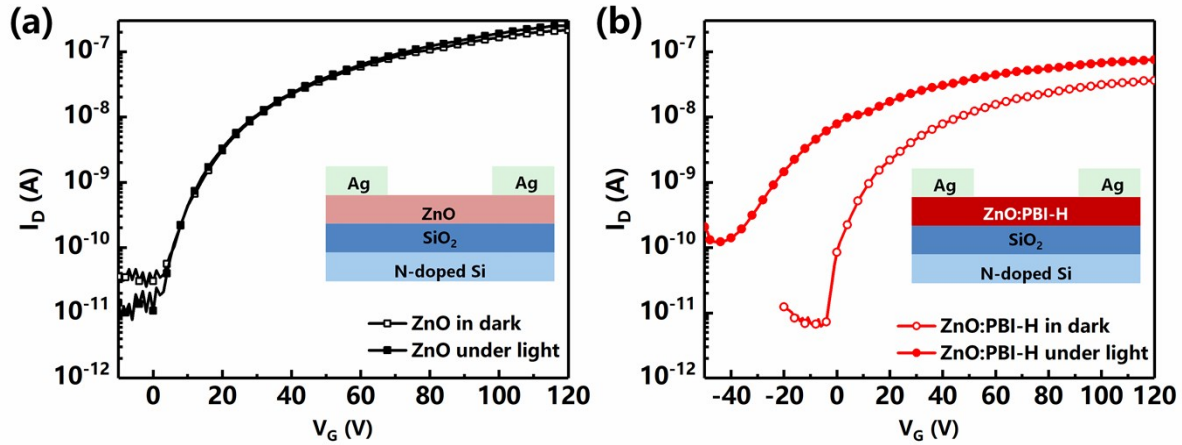


Fig. S9 Source-drain current versus gate voltage of (a) ZnO based FET and (b) ZnO:PBI-H based FET, respectively. The insert is the device structure of ZnO or ZnO:PBI-H based FET.

## 7. Contrast of fall time and schematic diagram for the charge transfer

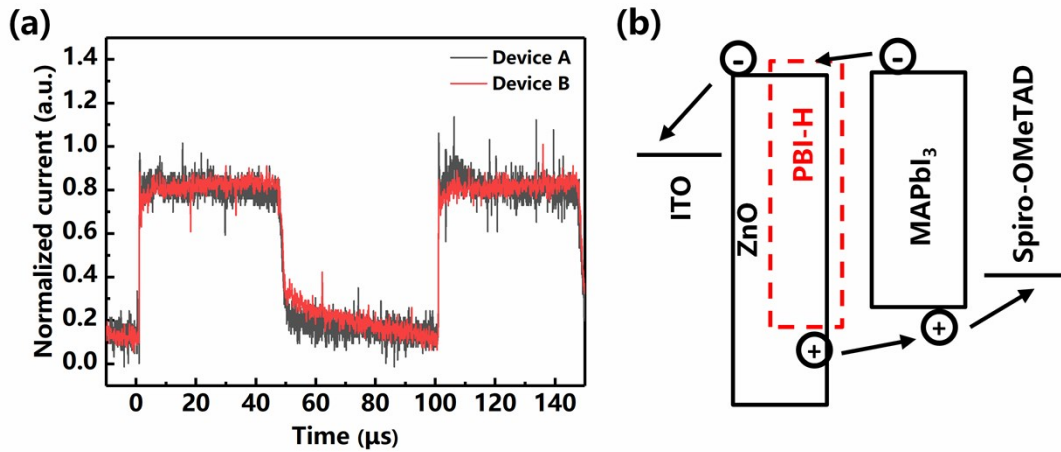


Fig. S10 (a) Response speed of Device A (black line) and Device B (red line); (b) Schematic diagram for the charge transfer between ZnO:PBI-H and perovskite when the laser turns off.

## 8. Response speed of devices with different active area

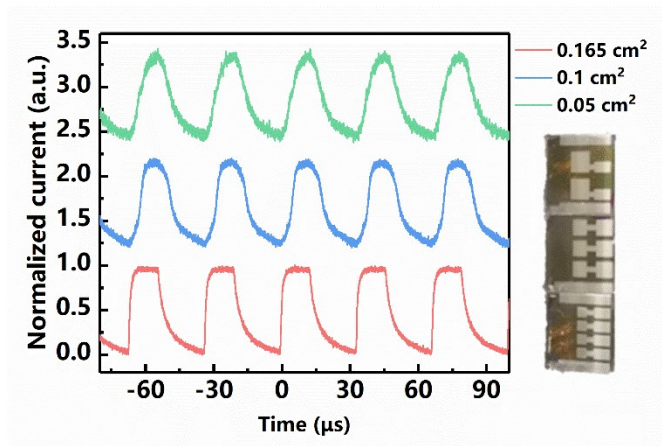


Fig. S11 Response speed of Device B with different active area measured at zero bias under the illumination of 633 nm laser modulated at the frequency of 30 kHz (square wave, 50% duty ratio). The insert is the photograph of devices with active area of 0.165, 0.1, and 0.05 cm<sup>2</sup> from top to bottom, respectively.

## 9. Summary of perovskite photodetectors with varied concentration of PEIE

Table S1. Summary of dark current, photocurrent, responsivity and detectivity of perovskite photodetectors with different interfacial layers.

Devices	Photocurrent density (mA·cm <sup>-2</sup> ) @ 0 V	Dark current density (mA·cm <sup>-2</sup> ) @ 0 V	Responsivity (A·W <sup>-1</sup> ) @ 0 V, 670 nm	Detectivity (Jones) @ 0 V, 670 nm
ZnO/0.2 wt% PEIE	18.4	$2.57 \times 10^{-6}$	0.34	$1.2 \times 10^{13}$
ZnO:PBI-H/0.1 wt% PEIE	16.4	$4.79 \times 10^{-6}$	0.31	$7.8 \times 10^{12}$

ZnO:PBI-H/0.2 wt% PEIE	18.7	$6.18 \times 10^{-7}$	0.35	$2.5 \times 10^{13}$
ZnO:PBI-H/0.3 wt% PEIE	8.1	$4.36 \times 10^{-7}$	0.20	$1.7 \times 10^{13}$
ZnO:PBI-H/0.4 wt% PEIE	1.1	$5.64 \times 10^{-7}$	0.02	$1.5 \times 10^{12}$

As shown in Table S1, the photocurrent density was much decreased with high concentration of PEIE solution, leading to the lower responsivity and detectivity. It should be noted that the dark current was measured by the Keithley 2400 source-meter (Tektronix), so there would be a little deviation in measuring such low dark current suppressed by PEIE at zero bias.

## 10. References

[S1] H. Zhou, Q. Chen, G. Li, S. Luo, T. B. Song, H. S. Duan, Z. Hong, J. You, Y. Liu and Y. Yang, *Science*, 2014, 345, 542-546.